A Photochemical Mechanism for Homochirogenesis. Part 2[§]

JOHN E. BARTMESS* AND RICHARD M. PAGNI
Department of Chemistry, University of Tennessee, Knoxville, Tennessee

ABSTRACT A theoretical investigation of the photochemistry of racemic compounds with circularly polarized light was undertaken. The exact solutions of the differential equations by numerical integration to the approximate solutions used in an earlier article were compared. The exact solutions showed that sequential reactions yield enhanced optical activities in the products. For irreversible reactions, all enantiomeric excesses are lost if the reactions are carried to completion, but appreciable resolution occurs in many cases for partial conversion. For reversible reactions, significant enantiomeric excesses are found at the photostationary state. *Chirality 25:16–21, 2013.*

KEY WORDS: photochemistry; kinetics; time-limited

INTRODUCTION

We have been interested for some time in developing mathematical models for the photochemistry of chiral molecules, both racemic and optically active, with unpolarized and circularly polarized light.[1–3] These models proved useful in understanding the photochemistry of racemic and optically active 2-iodooctane.[4–6] We recently turned our attention to a problem of great import.

One of the great unanswered questions in science, and one of great relevance to the origin of life, is how optically active molecules were formed in the prebiotic world.[7] Many theories have been proposed in the past to resolve this dilemma, but all of them have potentially serious problems.[8] New theories for the origin of homochirogenesis still appear regularly in the literature.[9,10] It is likely that photochemistry was a driving force for prebiotic synthesis in general.[11] Recently, we proposed a new photochemical mechanism using circularly polarized light, which is fairly common in interstellar space, that involves a sequence of photochemical reactions.[1] The premise for our proposal was that, if a single photochemical reaction yielded a small enantiomeric excess (ee) in the product, a sequence of two photochemical reactions would yield an even higher ee in the second photoproduct, a third photochemical reaction would yield a still higher ee, and so forth. This in fact is what we found. This theoretical model required the solution of a series of complex differential equations. The equations in general could only be solved analytically if one assumed that the total absorbance of the reactants and products was small at all times. This assumption, unfortunately, may not be reasonable in all cases even when a small number of molecules may be involved. For example, consider the one-step photochemical reaction $A \rightarrow P$, hereafter Scheme 1. Under the assumption that the Beer–Lambert law is valid, the following equations are exact:

$$\frac{d[A]}{dt} = -I\frac{S}{V}\frac{1-10^{-Ab}}{Ab}\varepsilon_A[\mathrm{A}]l\varphi_A \tag{1}$$

$$Ab = \varepsilon_A l[A] + \varepsilon_P l[P] \tag{2}$$

$$[A]o = [A] + [P] \tag{3}$$

where [A] and [P] are the concentrations of A and P, either during the reaction or initially, I is the light intensity in units of einstein $cm^{-2}\,s^{-1}$, S is the surface area of the reaction medium exposed to light in cm^2, V is the volume of the reaction medium in cm^3, Ab is the total absorbance of the medium, ε_A and ε_P are the extinction coefficients of A and P in $M^{-1}\,cm^{-1}$, l is the path length of the reaction medium in cm, and φ_A is the quantum yield of A reacting to give P. In passing, it is noted that $V = S^*l$. This results in the S/V term being cancelled by the l in the last term; however, l is still present in Ab, both in the denominator and exponent.

It is clear that the differential equation earlier will only be analytically solvable under very specific sets of conditions. For instance, if the absorbance of the medium is small, the differential equation earlier simplifies to[12]:

$$\frac{d[A]}{dt} = -I\ln 10\varepsilon_A[A]\varphi_A \tag{4}$$

which is an easily solvable first-order differential equation and notably independent of path length l. If only A absorbs radiation, i.e., $\varepsilon_P = 0$, the original differential equation is likewise solvable. If the absorbance is large, however, the first differential equation must be solved by numerical integration.

In the present article, we have two objectives: first, to compare the exact and approximate solutions of eqs. 1–4, and their equivalents in other reaction schemes, and to determine under what conditions the approximate solution holds. Does the approximate solution work for conditions that might be "real"? Second, to explore several photochemical schemes to see if any of them yield significant ees in the photoproducts. In all cases, we will use several criteria to assess the effectiveness of a photochemical scheme: ees of the products as a function of time, the yield of products as a function of time, and the difference in concentration of the enantiomers of each product as a function of time. We previously[1] focused only on the well-known ee function as the criterion for success in resolution. There is a problem with using the ee function this way; however, a large ee can occur without having an appreciable number of molecules of the excess enantiomer present. If the denominator of the ee formula is

*Correspondence to: John E. Bartmess, Department of Chemistry, University of Tennessee, Knoxville, Tennessee. E-mail: bartmess@utk.edu
[§]Part 1: Ref. 1
Received for publication 23 January 2012; Accepted 10 July 2012
DOI: 10.1002/chir.22105
Published online 11 September 2012 in Wiley Online Library (wileyonlinelibrary.com).

small, i.e., low concentration, then the ee can be large with only a modest concentration excess of one enantiomer. This has been shown to be the case in experimental work.[13] Likewise, another experimentally verified scenario is for a small ee to be amplified to a much larger one, via an autocatalytic sequence;[14] Breslow and Cheng have likewise shown[15] that a small ee in a compound such as an amino acid can be used to enhance significantly the ee of another compound such as a carbohydrate. In the present work, however, what is desired is production of a large concentration excess of one enantiomer over the other, starting from purely racemic material. In this work, the molar concentration difference between enantiomers, $[A_R]-[A_S]=\Delta_{R-S}[A]$, is adopted as the quantity to be examined, as a function of time and other parameters in these reaction schemes, in addition to ee.

We note that these schemes involve retention of stereochemistry at the chirality center, with the site of photochemistry different from that.

COMPUTATIONAL

The mechanistic schemes were evaluated by use of numeric integration of the given rate equations, to obtain the concentration versus time data shown in the figures. The numeric integrations were carried out on a conventional PC running Windows XP, using code written in Microsoft Fortran and with all key variables as double precision quantities. The figures presented here represent approximately 10^7–10^8 integration steps, but with only approximately 500 points plotted. Increasing or decreasing the step size by a factor of 1000 did not alter the numeric results to the fifth significant figure, indicating that under-integration and rounding errors are not problems.

RESULTS AND DISCUSSION

Because there are so many variables associated with the reaction schemes, a standard set of conditions, ideally close to what might occur in reality, is adopted. Only the variation from these will be noted in the results. Of the quantities seen in eqs. 1–3, typical values used are $\varepsilon=100\,M^{-1}cm^{-1}$, $[A]_0=1.0\,M$ with $[A_R]_0=[A_S]_0$, $l=0.001\,cm$, $V=0.001\,cm^3$, $S=1\,cm^2$, $I=5{\cdot}10^{-4}$ einstein $cm^{-2}s^{-1}$,[16] and $\varphi=1.0$. The ε, $[A]_0$, and l values yield a starting absorbance of 0.05. The other factors yield a pre-exponential term of -0.5 in eq. 1. Although we obviously cannot know the exact conditions that occurred for homochirogenesis, these values are reasonable for films of molecules under photoirradiation and more importantly result in 5–10 half-lives of data being plotted for the various mechanistic schemes evaluated here. That is sufficient to evaluate the schemes for their probability of generating an appreciable enantiomeric difference. These parameters correspond roughly to a half-life for eq. 1 of 18 h. As before,[1] the dissymmetry factor g is defined as $(\varepsilon_{AR}-\varepsilon_{AS})/([\varepsilon_{AR}+\varepsilon_{AS}]/2)$, where A_R and A_S are the R and S enantiomers of the starting racemic compound A. A typical g of 0.01 for a "normal" ε of 100 yields $\varepsilon_{AR}=99.5$ and $\varepsilon_{AS}=100.5$. Values of g up to 0.1 are known, e.g., for 3-methylcyclopentanone at 296 nm.[17]

The simplest reaction scheme that will allow some resolution is Scheme 1:

$$A_R \rightarrow P_R$$
$$A_S \rightarrow P_S,$$

where only A_R and A_S absorb. The kinetics are given by eqs. 1–4, with parallel equations for the R and S enantiomers. Using the typical conditions described earlier, we found the expected near-exponential fall of [A] and rise of [P]. These kinetic profiles are only near-exponential, because the presence of the absorbance Ab and thus [A] in the denominator means that the falloff with time will be slightly slower than the pure exponential function seen in the numerator. The deviation of the approximate solution from the exact one for [A] is found to be the largest immediately after time zero, and decreases thereafter. The standard conditions appear to be "low absorbance": the deviation is only 0.02% of [A] at the start. Because it is generally recognized[18] that experimentally determining relative concentration differences more precisely than 0.5% is very difficult, this deviation is not significant. What constitutes "high absorbance" therefore? From eq. 2, there are three variables that can lead to a high absorbance Ab: the extinction coefficient ε, the concentration [A], and the path length l. An examination of ε values of 100, 500, and 1000 results in larger deviations but still only proportionate to $1/\varepsilon$: it takes $\varepsilon=5000$ to result in a deviation of 0.5%, which corresponds to $Ab=2.5$. Likewise, the path length l in the absorbance needs to be greater than 0.05 cm to result in a deviation of $>0.5\%$.

More intriguing is the difference between the ee and the molar concentration difference $\Delta_{R-S}[A]$ in this case. In Figure 1, it is seen that the ee increases near linearly with time under the standard conditions ($l=0.001$, upper solid line), although at long time, the high ee represents only a small $\delta[A]$. The $\Delta_{R-S}[A]$ function (lower solid line), in contrast maximizes at approximately 1.4 half-lives, at 0.00184 M $(\equiv)_{R-S}[A]_{max}$). The half-life cited is only approximate, due to the non-exact exponential nature of $d[A]/dt$. This is a key result: even the simplest kinetic scheme can yield real resolution of racemic starting material, if done under the proper time-limited irradiation conditions. Decreasing l results in little visible change to the plot; increasing it to 0.01, as shown in the dashed line on the plot, results in a curved ee behavior, which actually becomes larger than the ee for $l=0.01$ at times beyond those shown on the plot. $\Delta_{R-S}[A]_{max}$ occurs at longer time, although still roughly 1.4 half-lives, but has the same value regardless of the value of l. Note that this also implies at the time that there is a $\Delta_{R-S}[P]$ of equal but opposite sign

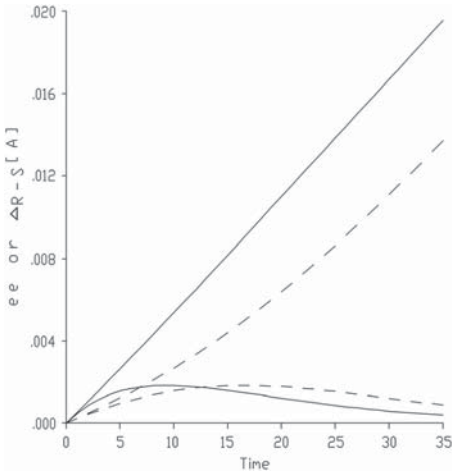

Fig. 1. Scheme 1, enantiomeric excess (ee) (upper lines) and $\Delta_{R-S}[A]$ (lower lines) for $l=0.001$ (solid lines) and $l=0.01$ (dashed lines).

for a total excess enantiomer content of $2 \times 0.00184\,\mathrm{M} = 0.00368\,\mathrm{M}$ at the time of maximum $\Delta_{R-S}[\mathrm{A}]$.

Two other situations were evaluated for Scheme 1. Varying the g values from 0.01 to 0.1 ($\varepsilon_{AR} = 95.0$; $\varepsilon_{AS} = 105.0$) and to 0.002 ($\varepsilon_{AR} = 99.9$; $\varepsilon_{AS} = 100.1$) results in plots of essentially the same appearance as Figure 1 for $l = 0.001$. However, $\Delta_{R-S}[\mathrm{A}]_{max}$, although occurring at the same time as for Figure 1, was 10 times as large in concentration for $g = 0.1$ and 0.2 times as large for $g = 0.002$, directly proportional to the g value. Secondly, varying the ε values up to 1000 or down to 50, at constant $g = 0.01$, results in a constant $\Delta_{R-S}[\mathrm{A}]_{max}$ value but at proportionate delay times. The timing of the maximum is still at approximately 1.4 half-lives in terms of $d[\mathrm{A}]/dt$.

The next more elaborate mechanistic scheme, hereafter Scheme 2, involves the sequence of reactions:

$$\mathrm{A}_S \rightarrow \mathrm{B}_S \rightarrow \mathrm{P}_S$$
$$\mathrm{A}_R \rightarrow \mathrm{B}_R \rightarrow \mathrm{P}_R$$

where both A and B absorb differentially by enantiomer and P does not absorb. The kinetics are described by

$$\frac{d[A_S]}{dt} = -I\frac{S}{V}\frac{1-10^{-Ab}}{Ab}\varepsilon_{A_S} l[A_S]\varphi_A \quad (5)$$

$$\frac{d[B_S]}{dt} = I\frac{S}{V}\frac{1-10^{-Ab}}{Ab}\varepsilon_{A_S} l[A_S]\varphi_A - I\frac{S}{V}\frac{1-10^{-Ab}}{Ab}\varepsilon_{B_S} l[B_S]\varphi_B \quad (6)$$

$$Ab = \varepsilon_{A_R} l[A_R] + \varepsilon_{A_S} l[A_S] + \varepsilon_{B_R} l[B_R] + \varepsilon_{B_S} l[B_S] \quad (7)$$

$$\frac{1}{2}[A]_0 = [A_S] + [B_S] \quad (8)$$

$$\frac{1}{2}[A]_0 = [A_R] + [B_R] \quad (9)$$

with equivalent equations to 5 and 6 for the R enantiomers. For this scheme, the effect of different values for g_A and g_B was tested, as presented in Table 1.

Figure 2, although for set 1, shows the pattern of abundances for all five sets and is typical of that for sequential first-order reactions.[18] This is consistent with the fact that the average extinction coefficient $(\varepsilon_{AR} + \varepsilon_{AS})/2$ is equal to 100 in all cases; only g values are being varied here, and thus, $[\mathrm{B}]_{max}$ and the points where [A] = [P], and where [B] reaches a maximum, are essentially the same for all sets.

Likewise, Figure 3, of ee versus time for set 1, shows similarities to those quantities in Scheme 1: the maximum ee for A and B are at long times, where their concentrations are very

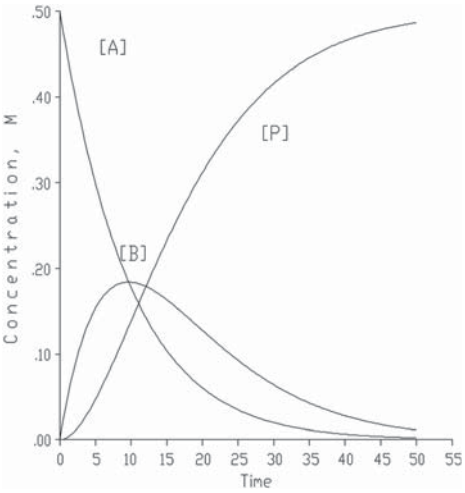

Fig. 2. Time dependence of concentrations for Scheme 2.

TABLE 1. Conditions for different evaluations of Scheme 2[a]

Set	1	2	3	4	5
g_A	0.01	0.01	0.1	0.01	0.002
g_B	0.01	−0.01	0.01	0.002	0.01
$[\mathrm{B}]_{max}$[b]	0.18394	0.18302	0.1797	0.18357	0.18431
$t,[\mathrm{B}]_{max}$	9.7	9.6	9.9	9.6	9.6
[A] = [P][c]	0.15795	0.15797	0.1598	0.15797	0.157245
$t,$[A] = [P]	11.1	11.1	11.5	11.1	11.1
$\Delta_{R-S}[\mathrm{A}]_{max}$[d]	0.001839	0.001839	0.0184	0.001839	0.000368
$t(\Delta_{RS}[\mathrm{A}]_{max})$	9.6	9.6	9.6	9.6	9.6
$\Delta_{R-S}[\mathrm{B}]_{min}$[e]	−0.00081	0	−0.01107	−0.00106	−0.000071
$t(\Delta_{R-S}[\mathrm{B}]_{min}$	3.7	0	5.4	5.1	1.5
$\Delta_{R-S}[\mathrm{B}]_{max}$[f]	0.001545	0	0.004956	0.000601	0.001365
$t(\Delta_{RS}[\mathrm{B}]_{max})$	24.4	0	30.2	29.1	20.5
$\Delta_{R-S}[\mathrm{P}]_{min}$[g]	−0.00271	0	−0.01499	−0.00162	−0.001624
$\mathrm{t}(\Delta_{R-S}[\mathrm{P}]_{min})$	18.9	0	18.9	18.9	18.9
$\Delta_{R-S}[\mathrm{T}]_{max}$[h]	0.005412	0.003679	0.036803	0.003679	0.003248
$\mathrm{t}(\Delta_{RS}[\mathrm{T}]_{max})$	18.9	9.6	9.6	9.6	18.9

[a]For all sets: $\varepsilon_A = \varepsilon_B = 100$. Other conditions are the "standard" ones from the text.
[b]Maximum concentration point of [B] in Figure 2.
[c]Concentration at point of crossing of A and P lines in Figure 2.
[d]Maximum value of $\Delta_{R-S}[\mathrm{A}]$ in Figure 5.
[e]Minimum value of $\Delta_{R-S}[\mathrm{B}]$ in Figure 5.
[f]Maximum value of $\Delta_{R-S}[\mathrm{B}]$ in Figure 5.
[g]Minimum value of $\Delta_{R-S}[\mathrm{P}]$ in Figure 5.
[h]Point of maximum chirality in Figure 5, see text.

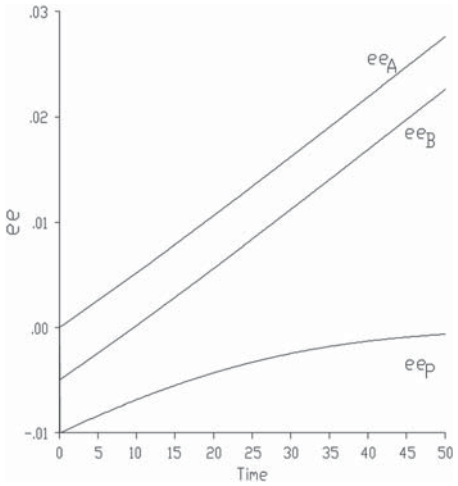

Fig. 3. Time dependence of ee for Scheme 2, for set 1 ($g_A = g_B$) in Table 1.

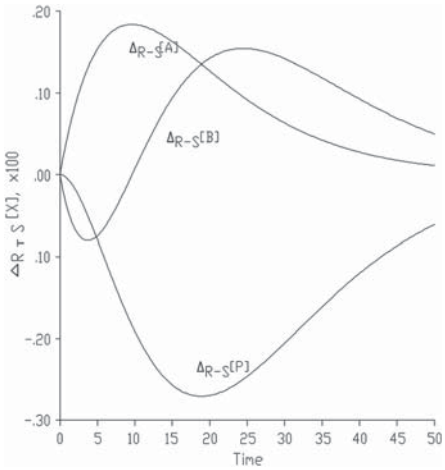

Fig. 5. Time dependence of molar enantiomer difference Δ_{R-S}[A] and others for Scheme 2, set 1 ($g_A = g_B$).

small, and the ee for P approaches zero at those times, when its concentration is large. Only for set 2, where g_A and g_B are equal but of opposite sign, is a different pattern seen, as in Figure 4: the ee plot has ee_P as 0 at all times, ee_B as constant at −0.005 at all times, and ee_A increasing.

Figure 5 shows the Δ_{R-S}[A], Δ_{R-S}[B], and Δ_{R-S}[P] values versus time for set 1 and is of the same general shape as those for sets 3–5. Figure 6 is for set 2 where $g_A = -g_B$. In all five sets, the maximum value for Δ_{R-S}[δ[A] occurs at the time where [B] maximizes in Figure 2. The extremes in value of Δ_{R-S}[B] and δ[Δ_{R-S}[P] vary with the conditions. In Table 1 is also noted the maximum value and time of δ[T] = Δ_{R-S}[A] + Δ_{R-S}[B] + Δ_{R-S}[P], where the total chirality T is maximized. It is evident that this is roughly a function of the sum of the absolute g values, but not a simple one. The special case of Figure 6, where $g_A = -g_B$, is noteworthy. Although at no time is there any resolution of the final product, due to the cancellation of the differential absorbances in the two successive steps, quite appreciable resolution of A and B is observed at times comparable with the more additive cases.

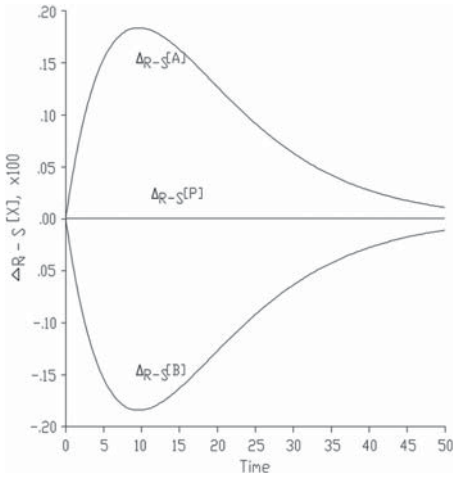

Fig. 6. Time dependence of molar enantiomer difference Δ_{R-S}[A] and others for Scheme 2, set 2 ($g_A = -g_B$).

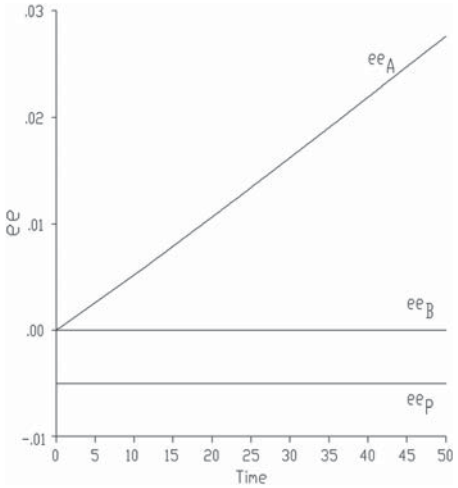

Fig. 4. Time dependence of enantiomeric excess (ee) for Scheme 2, for set 2 ($g_A = -g_B$) in Table 1.

We thus see that even for the simplest Scheme 1, or for Scheme 2 where there is no net differential absorbance over two steps, substantial resolution is observed at intermediate times.

Another case of interest is the photostationary state shown in Scheme 3. Alkene photoisomerization is a well-known case of a photostationary state, where the steady-state concentrations of the reactant and product differ appreciably from the thermal equilibrium value.[19] It is assumed here that A_R interconverts only with B_R, and A_S only with B_S, but that the ε and g values for A and B can be different.

Scheme 3:

$$A_R \underset{h\nu}{\overset{h\nu}{\rightleftharpoons}} B_R$$

$$A_S \underset{h\nu}{\overset{h\nu}{\rightleftharpoons}} B_S$$

The kinetics are described by eqs. 5–9 for Scheme 2, save that eq. 10 replaces eq. 5.

$$\frac{d[As]}{dt} = I\frac{S}{V}\frac{1-10^{-Ab}}{Ab}\varepsilon_{BS}l[Bs]\varphi_B - I\frac{S}{V}\frac{1-10^{-Ab}}{Ab}\varepsilon_{AS}l[As]\varphi_A \quad (10)$$

There will of course be another pair of equations of the same form as 6 and 10, involving the *R* enantiomers. The steady-state ratio, assuming unit quantum yield in both directions, is set by the relative average ε values of A and B, so $[B]_{PS}/[A]_{PS} = \varepsilon_A/\varepsilon_B$ where PS means the long-time photostationary state. The species with the smaller ε is favored at long times.

Starting from pure racemic A, the time dependence of the concentrations is as expected for a simple approach to equilibrium: A falls approximately exponentially, and B rises, to their steady-state concentrations. The $\Delta_{R-S}[A]$ and $\Delta_{R-S}[B]$ values are more interesting and are dependent on the *g* values. For $g_A/g_B = 1.0$, behavior such as in Figure 7 is observed: appreciable $\Delta_{R-S}[A]$ and $\Delta_{R-S}[B]$ at some intermediate time but falling to zero at long times. However, for $g_A < g_B$ or the reverse, Figure 8 with $g_A/g_B = 0.1$ shows that $\Delta_{R-S}[A]$ and $\Delta_{R-S}\delta[B]$ "maximize" at long times. By setting the derivative in eq. 10 to 0, to represent the steady-state condition at infinite time, and then solving with eq. 8 plus the equivalent equations for the *R* enantiomer, it can be shown that $\Delta_{R-S}[A]_{PS}$ is given by eq. 11:

$$\Delta_{R-S}[A]_{PS} = \frac{[A]_0}{2}\left[\frac{\varepsilon_{Br}}{(\varepsilon_{Ar}+\varepsilon_{Br})} - \frac{\varepsilon_{Bs}}{(\varepsilon_{As}+\varepsilon_{Bs})}\right] \quad (11)$$

As seen in Table 2, Scheme 3 can thus result in appreciable enantiomeric enrichment without the time-critical behavior seen previously for the other schemes. This is also a case where ee does reflect enantiomeric enrichment, because the concentrations of A and B are nonzero at long times.

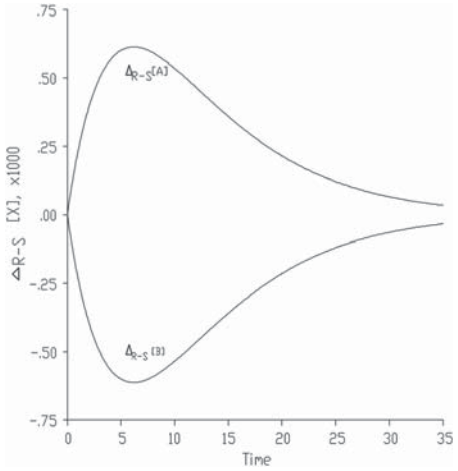

Fig. 7. Time dependence of molar enantiomer difference $\Delta_{R-S}[A]$ and $\Delta_{R-S}[B]$ for Scheme 3, $g_A = g_B$.

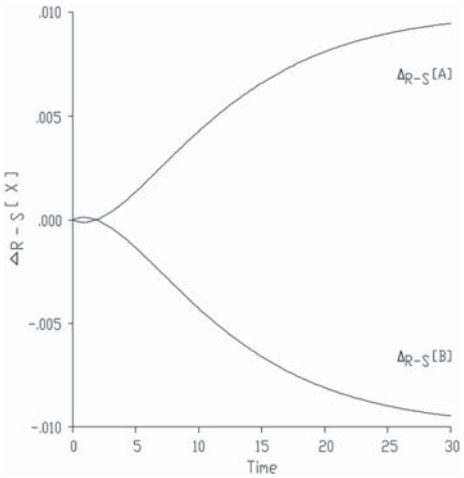

Fig. 8. Time-dependence of molar enantiomer difference $\Delta_{R-S}[A]$ and $\Delta_{R-S}[B]$ for Scheme 3, $g_A = g_B/10$.

CONCLUSIONS

The aforementioned models for homochirogenesis via photochemical reactivity with circularly polarized light indicate that (1) under believable conditions, the exact and approximate solutions are similar in value; (2) schemes with more than one step can yield higher total chirality; and (3) reversible reactions, notably the photostationary state, are interesting because enantiomeric differences are not lost if reactions run to completion. Regardless of the reasonableness of the model, is this a possible mechanism in reality? Because our Sun does not afford much circularly polarized light at the surface of the earth, the best options for making optically active molecules photochemically on the earth are either via a neutron star passing close to the solar system several billion years ago or a meteor passing through the light cone of a neutron star long ago and then crashing to earth and depositing the prebiotic molecules on the earth. For the former case, the prebiotic atmosphere's lack of O_2 should allow higher energy photons to reach the surface of the earth compared with the present, favoring energetic photochemistry at the surface. In support of the latter possibility, the Murchison meteorite contained a slew of optically active amino acids.[20] A potential synthesis sequence is the formation of racemic multi-stereocenter carbohydrates via cold photolysis of formaldehye[21] followed by selective photodestruction of one enantiomer over the other via circularly polarized light.[22] Such scenarios provide the time-resolved irradiation necessary to achieve resolution via Schemes 1 and 2. As noted, Scheme 3 need not be time-resolved to achieve appreciable resolution.

It is clear from this and our earlier work that it is theoretically possible to enhance small ees obtained in a single photochemical reaction with circularly polarized light by a sequence of two or more such photoreactions. There are, not surprisingly, other methods in which the enhancement

TABLE 2. Steady-state enantiomer difference $\Delta_{R-S}[A]_{PS}$ for Scheme 3[a]

	$\varepsilon_A/\varepsilon_B$:	50/100	100/100	100/50
g_B:	g_A/g_B	$\Delta_{R-S}[A]_{PS}$	$\Delta_{R-S}[A]_{PS}$	$\Delta_{R-S}[A]_{PS}$
0.100	0.1	−0.01001	−0.01126	−0.01000
0.020	0.5	−0.00111	−0.00125	−0.00111
0.010	1.0	0.00000	0.00000	0.00000
0.002	5.0	0.00088	0.00100	0.00088
0.001	10.	0.00100	0.00112	0.00100

[a] $l = 0.001$, $g_A = 0.01$, $[A_R]_0 = [A_S]_0 = 0.5$ M for all. $\Delta_{R-S}[A]_{PS}$ from eq. 11.

can be accomplished. Kawasaki *et al*. have shown experimentally that a very small enhancement in ee obtained in a single photochemical reaction can be further enhanced to close to enantiomeric purity using the Soai reaction,[23] although it is hard to imagine that the use of diisopropylzinc, a prerequisite in the Soai reaction, has any prebiotic relevance.

ACKNOWLEDGMENT

We thank Prof. Ron Breslow for helpful discussions.

LITERATURE CITED

1. Pagni RM, Bartmess JE. A photochemical mechanism for homochirogenesis. J Phys Chem A 2007;111:10604–10608.
2. Pagni RM, Bartmess JE. Theoretical insights into photochemical reactions initiated with circularly polarized light. Chirality 2006;18:419–425.
3. Pagni RM, Bartmess JE. Photoreaction of a racemate proceeding through radical or ion pairs. The effect of circularly polarized light on the enantiomeric excess of recovered reactant. Chirality 2003;15:772–776.
4. Gao F, Boyles D, Sullivan R, Compton RN, Pagni RM. Photochemistry of racemic and resolved 2-iodooctane. Effect of solvent polarity and viscosity on the chemistry. J Org Chem 2002;67:9361–9367.
5. Gao F, Compton RN, Pagni RM. The multiphoton photochemistry of 2-iodooctane in methanol. Chem Commun 2003;1584–1585.
6. Conley-Murphy N, Compton RN, Pagni, RM. The photochemistry of racemic and optically active 2-iodooctane in acetonitrile - water mixtures. Prog React Kinet Mech 2010;35:81–92.
7. Scaife C. What is the universe made of? Science 2005;309:78–78.
8. Compton RN, Pagni RM. The chirality of biomolecules. Adv Atom Mol Opt Phys 2002;48:219–261.
9. Boyd RN, Kajino T, Onaka T. Supernovae and the chirality of the amino acids. Astrobiol 2010;10:561–568.
10. Kim SK, Ha T, Schermann JP. Editorial. Phys Chem Chem Phys 2011;13:804–805.
11. Schrader ME. The RNA world: conditions for prebiotic synthesis. J Geophys Res 2009;114:D15305-15311.
12. Mauser H, Gauglitz G. Photokinetics. Theoretical Fundamentals and Applications. In: Compton RG, Hancock G, editors. Comprehensive chemical kinetics. Amsterdam: Elsevier; 1998, Ch. 3. p 191–217.
13. Balavoine, Moradpour A, Kagan H. Preparation of chiral compounds with high optical purity by irradiation with circularly polarized light, a model reaction for the prebiotic generation of optical activity. J Am Chem Soc 1974;96:5152–5158.
14. Soai K, Shibata T, Morioka H, Choji K. Asymmetric autocatalysis and amplification of enantiomeric excess of a chiral molecule. Nature 1995;378:767–768.
15. Breslow R, Cheng Z-L. L-amino acids catalyze the formation of an excess of D-glyceraldehyde, and thus of other D sugars, under credible prebiotic conditions. Proc Nat Acad Sci 2010;107:5723–5725.
16. Grant RH, Slusser JR. Estimation of photosynthetic photon flux density from 368-nm spectral irradiance. J Atmos Ocean Tech 2003;21:481–487.
17. Bertucci C, Andrisano V, Carrini V, Castiglioni E. Reliable assay of extreme enantiomeric purity values by a new circular dichroism based HPLC detection system. Chirality 2000;12:84–92.
18. Frost AA, Pearson RG. Kinetics and mechanism, 2nd ed. New York: Wiley; 1961. p 166–169.
19. Waldeck DH. Photoisomerization dynamics of stilbenes. Chem Rev 1991;91:415–436.
20. Engel MH, Nagy B. Distribution and enantiomeric composition of amino acids in the Murchison meteorite. Nature 1982;296:837–837.
21. Yamauchi M, Ahmed SN. Formation of carbohydrates by the photolysis of formaldehyde. J Undergrad Chem Res 2003;1:29–32.
22. Shimizu Y. Laser-induced enantioenrichment of tartaric acid via a multiphoton absorption process. J Chem Soc Perkin Trans I 1997;1275–1278.
23. Kawasaki T, Sato M, Ishiguro S, Saito T, Morishita Y, Sato I, Nishino H, Inoue Y, Soai K. Enantioselective synthesis of near enantiopure compound by asymmetric autocatalysis triggered by asymmetric photolysis with circularly polarized light. J Am Chem Soc 2005;127:3274–3275.